

Subdivision Surfaces Based on Point-Based Splines

Wenming Zhu Jiansong Deng Falai Chen
Department of Mathematics
University of Science and Technology of China
Hefei, Anhui 230026, P. R. of China

Abstract

We present a new interpolatory subdivision scheme based on PB-splines (Point-Based B-splines), over triangular meshes. Using the stencil of the interpolatory $\sqrt{3}$ -subdivision scheme, we propose a different refinement strategy by introducing a variable α to each regular vertex (valence = 6). By applying different α (locally or globally), the scheme is suitable for adaptive refinement and can perfectly reach different smoothness conditions (C^0 , C^1 or C^2).

1. Introduction

Given a subdivision scheme, a sequence of refined meshes M_1, M_2, \dots, M_n can be computed from the initial coarse control mesh M_0 . This sequence of meshes converges eventually to a continuous limit smooth surface M_∞ .

Many subdivision surface schemes have been proposed in the last decade. Some are based on tensor-product surface generation schemes [1, 3] and some are from 2-scale relations in a more general functional space defined over three-directional grids [4, 9, 11]. Due to the nature of refinement operators, the generalized tensor-product schemes naturally lead to quadrilateral meshes while the others lead to triangular meshes. In case of subdivision methods over triangular mesh, the so called 1-to-4 split operation is most popular which is implemented by introducing a new vertex on each edge [4, 9] while face-split operation is also developed in the recent 10 years [5].

In 2000, L. Kobbelt introduced a new approximate subdivision scheme, known as $\sqrt{3}$ -subdivision, over triangular mesh [6]. In that scheme, for each triangle of the coarser mesh, its barycenter is computed and new topology is generated by connecting each vertex of the triangle and the inserted point and then flipping all old edges of the mesh. After each two steps of the $\sqrt{3}$ -subdivision scheme, every triangle is subdivided into 9 sub-triangles and every edge is split into 3 sub-edges, which leads to the name $\sqrt{3}$ -subdivision. U. Labsik and G. Greiner [7] proposed the

interpolatory version of $\sqrt{3}$ -subdivision scheme in which the generalization of a one-dimensional cubic interpolatory polynomial $p_3(x)$ for given points $f(0), f(1), f(2), f(3)$ is considered. The stencil of the interpolatory $\sqrt{3}$ -subdivision scheme uses one triangle and its 1-neighbor triangles, which has 12 vertices in the lump.

We present a subdivision scheme using the analog stencil as the interpolatory $\sqrt{3}$ -subdivision scheme but a different approach to generate weights. Here we consider a family of splines called *Point-Based Spline* [10] defined over a triangular mesh. The spline we used is a piecewise-quartic (or higher degree) function. New vertex added in the triangle is computed by the combination of *PB-splines* of the vertices over the stencil. The advantages of this scheme are that only split operation is needed during each subdivision step, and that the smoothness of the mesh can be controlled to satisfy different continuity requirement from C^0 to C^2 . This can be done by introducing a variable α to each regular vertex of the mesh.

The paper is organized as follows. In Section 2, we give a review of interpolatory subdivision schemes, especially interpolatory $\sqrt{3}$ -subdivision scheme. In Section 3, PB-spline over triangular mesh is introduced. Sections 4, and 5 describe our subdivision scheme based on PB-splines in detail. In Sections 6 and 7 we present some examples and draw a conclusion.

2. Interpolatory subdivision schemes

The Butterfly subdivision is a famous interpolatory subdivision scheme over triangular meshes. In the Butterfly scheme, an 8-point stencil is used to compute a new vertex on an edge over a regular triangular mesh where all vertices have valence 6 (See Figure 1.a).

Given the result of k -th subdivision step, the position of new vertex q^{k+1} is computed as follows

$$q^{k+1} = \frac{1}{2}(p_1^k + p_2^k) + 2w(p_3^k + p_4^k) - w(p_5^k + p_6^k + p_7^k + p_8^k), \quad (1)$$

where w is a tension parameter normally set to $1/16$. Considered as a scalar valued function over a three directional grid, when the function value is constant along one of these directions, the Butterfly scheme reduces to a 4-point scheme

$$q^{k+1} = \left(\frac{1}{2} + w\right)(p_i^k + p_{i+1}^k) - w(p_{i-1}^k + p_{i+2}^k) \quad (2)$$

along the other two directions [7] and the generalization of this 4-point scheme leads to the interpolatory $\sqrt{3}$ -subdivision (See Figure 1.b).

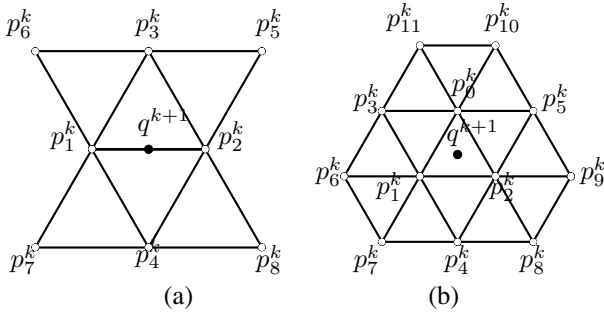


Figure 1. Stencil of the Butterfly scheme (a) and interpolatory $\sqrt{3}$ -subdivision scheme (b)

In this 12-point stencil, a new point is computed as

$$q^{k+1} = a(p_0^k + p_1^k + p_2^k) + b(p_3^k + p_4^k + p_5^k) + c(p_6^k + p_7^k + p_8^k + p_9^k + p_{10}^k + p_{11}^k). \quad (3)$$

The parameters a, b, c can be derived from equation

$$p\left(\frac{5}{3}\right) = -\frac{4}{81}f(0) + \frac{20}{27}f(1) + \frac{20}{27}f(2) - \frac{5}{81}f(3), \quad (4)$$

where $p(x)$ is a cubic polynomial interpolating four given points $f(0), f(1), f(2), f(3)$ [7]. By evaluating the equation above, we get $a = \frac{32}{81}, b = -\frac{1}{81}$ and $c = -\frac{2}{81}$.

3. Point-based splines

Thomas W. Sederberg *et al* proposed point-based (PB) spline over rectangular grids in [10]. This type of tensor-product PB-spline is defined as

$$\mathbf{P}(s, t) = \sum_{i=1}^n \mathbf{P}_i B_i^n(s, t) / \sum_{i=1}^n B_i^n(s, t), \quad (5)$$

where \mathbf{P}_i are control points and $B_i^n(s, t)$ is the basis function given by

$$B_i^n(s, t) = M_{i0}^3(s) N_{i0}^3(t),$$

where $M_{i0}^3(s)$ is the cubic B-spline function associated with knot vector $s_i = [s_{i0}, s_{i1}, s_{i2}, s_{i3}, s_{i4}]$ and $N_{i0}^3(t)$ is the cubic B-spline function associated with knot vector $t_i = [t_{i0}, t_{i1}, t_{i2}, t_{i3}, t_{i4}]$.

Sederberg's PB-splines are defined over rectangular domain. In this paper, we propose a new PB-spline defined over a regular triangular parametric domain \mathbb{D} . The basis function $P_i(u, v, w)$, with barycentric coordinate (u, v, w) , is a piecewise polynomial which is constructed as follows. First, a 1-disc basis function $D_i(u, v, w)$ is defined over the 1-neighborhood of each vertex p_i, Ω_i (Union of all triangles around p_i , See Figure 2.a).

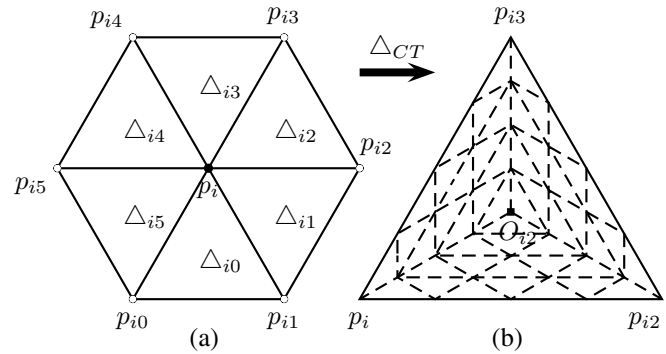


Figure 2. Ω_i (a) and the Clough-Tocher split over triangle Δ_{i2} (b)

A piecewise Bézier function $F_{ij}(u, v, w)$ of degree $N \geq 4$ is defined over the macro-elements of Clough-Tocher(CT) split [2] for each triangle $\Delta_{ij} \subset \Omega_i, j = 0, \dots, 5$. In Figure (2.b), we show the CT split for $j = 2$. It should be noted that the value of F_{i2} is 1 at $p_i, \frac{1}{3}$ at barycenter O_{i2} and 0 along the boundary $p_{i2}p_{i3}$. More constraints should be added to maintain the $C^1(G^1)$ smooth boundary conditions between Δ_{i2} and its neighbor (Δ_{i1}, Δ_{i3} and outside Ω_i respectively). [8]. By applying above procedure to each triangle in Ω_i , we get a piecewise Bézier function D_i of degree N over \mathbb{D} which has local support Ω_i (See Figure 3.a) and

$$D_i|_{\Delta_{ij}} = F_{ij}, j = 0, \dots, 5.$$

The 1-disc PB basis functions D_i have the following advantages:

1. $0 \leq D_i(u, v, w) \leq 1$ for any $(u, v, w) \in \mathbb{D}$, and $D_i \equiv 0$ on $\mathbb{D} \setminus \Omega_i$;
2. $D_i|_{p_i} = 1$ and $D_i|_{O_{ij}} = 1/3$ for $j = 0, \dots, 5$ and any i , where O_{ij} is the barycenter of triangle Δ_{ij} .
3. $\sum_i D_i \equiv 1$ over \mathbb{D} if all triangles are equilateral.

Now the 1-disc PB-spline can be defined as

$$D(u, v, w) = \sum_i c_i D_i(u, v, w) / \sum_i D_i(u, v, w). \quad (6)$$

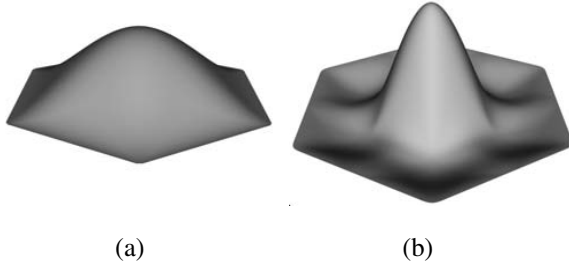


Figure 3. 1-Disc (a) and 2-Disc (b) PB spline

We note that the value of $\sum_i D_i$ at the barycenter of triangle $\triangle p_i p_j p_k$ depends on only three basis functions: D_i , D_j and D_k , i.e., $D_i|_p = D_j|_p = D_k|_p = 1/3$. When applied to generate a subdivision scheme in 3-dimensional space by adding a new point at its barycenter $u = v = 1/3$, it is easy to verify that the new point is coplanar with the vertices p_i , p_j , p_k , thus the ‘refinement’ operation has no effects on the coarser mesh.

To overcome above limits, we extend the 1-disc PB-splines to 2-disc PB-splines which need 2-neighborhood of a vertex and use a parameter α to combine the 1-disc PB-splines.

The 2-disc PB-spline basis function $P_i(u, v, w)$ over triangular domain \mathbb{D} can be written as

$$P_i(u, v, w) = D_i(u, v, w) + \alpha \sum_{j=0}^5 D_{ij}(u, v, w), \quad (7)$$

where $D_i(u, v, w)$, $\{D_{ij}\}_{j=0}^5$ is the 1-disc PB-spline basis function of vertex p_i and its 1-neighbor $\{p_{ij}\}_{j=0}^5$ respectively. Now function P_i is 1 at p_i , α at 1-neighbor vertices $\{p_{ij}\}_{j=0}^5$, and constant 0 outside the 2-neighborhood (See Figure 3.b). Moreover, P_i has some nice properties:

1. If triangles in domain \mathbb{D} are all equilateral triangles, $\sum_{i \in \mathbb{Z}} P_i(u, v, w) \equiv 1 + 6\alpha$, for any $(u, v, w) \in \mathbb{D}$.
2. $P_i(u, v, w)$ is a C^2 continuous Bézier function over each macro-element of Clough-Tocher split of domain \mathbb{D} and C^1 continuous on the boundary of each macro-element, as well as C^1 continuous along the boundary of the whole support.

Now a 2-disc PB-spline of degree N ($N \geq 4$) over a triangular domain can be written as

$$\mathbf{P}(u, v, w) = \sum_i c_i P_i(u, v, w) / \sum_i P_i(u, v, w). \quad (8)$$

In the next section we will propose a subdivision scheme over triangular mesh based on 2-disc PB-splines.

4. Subdivision scheme

The new point added to each triangle during one step of subdivision is the linear combination of all points whose 2-disc splines influence the triangle. Therefore a 12-point stencil is needed when computing a new point (See Figure 1.b).

From the stencil and the properties of PB-spline we know that $\sum_i P_i|_p = 1 + 6\alpha$, where p is the barycenter of any triangle domain. So given heights h_i over each vertex of the stencil, the height of p , say h , is computed as

$$h = \left(\sum_{i=0}^{11} h_i P_i|_p \right) / (1 + 6\alpha), \quad (9)$$

where $P_i|_p$ can be derived from equation (7) as

$$\begin{aligned} P_0|_p &= P_1|_p = P_2|_p = (1 + 2\alpha)/3, \\ P_3|_p &= P_4|_p = P_5|_p = 2\alpha/3, \\ P_i|_p &= \alpha/3, \quad i = 6, \dots, 11. \end{aligned} \quad (10)$$

Given the control mesh $M_k \subset \mathbb{R}^3$ of the k -th subdivision step, we now generate the $(k + 1)$ -th finer mesh M_{k+1} by introducing a point to each triangle of M_k . To do so, we first find the stencil in which all vertices are regular (valence = 6), and then we determine the new point q^{k+1} by the following equation

$$q^{k+1} = a(p_0^k + p_1^k + p_2^k) + b(p_3^k + p_4^k + p_5^k) + c \sum_{i=6}^{11} p_i^k, \quad (11)$$

where p_i^k is the vertex on $M_k \subset \mathbb{R}^3$, and

$$a = (1 + 2\alpha)/(3 + 18\alpha), \quad c = \alpha/(3 + 18\alpha), \quad b = 2c.$$

Obviously this scheme leads to C^0 continuous limit surface since $3a + 3b + 6c \equiv 1$ for any parameter $\alpha \in \mathbb{R} \setminus \{-1/6\}$, while a, b, c have no definition for $\alpha = -1/6$. The subdivision matrix S of the scheme, which has a size of 37×37 and whose elements are determined by equations (11), maps a certain region of M_k to a ‘scaled’ region in the $(k + 1)$ -th mesh M_{k+1} . L. Kobbelt [6] suggests to use matrix $\tilde{S} = RSS$ instead of S to analyze the convergence of the scheme where R is a permutation matrix. The eigen-analysis of matrix $\tilde{S} = RSS$ shows that the scheme is convergent and leads to C^1 limit surfaces if the leading eigenvalues of \tilde{S} are

$$\lambda_0 = 1, \quad \lambda_1 = \lambda_2 = 1/3, \quad |\lambda_i| < 1/3, \quad i = 3, \dots, 36.$$

For our scheme, these conditions are satisfied for any $\alpha \in (-0.08, -0.025)$ by computing the eigenvalues of \tilde{S} numerically.

We also analyze the behavior of the difference scheme of 6-ring subdivision matrix which is the size of 127×127 [6], and we have numerically proved that the largest singular value of the 3rd directional difference matrix S_n is less than $1/9$ when $\alpha \in (-0.056, -0.032)$, i.e.,

$$3^2 \| S_n(\alpha) \| < 1,$$

which means our subdivision scheme is C^2 convergent for any parameter $\alpha \in (-0.056, -0.032)$.

5. Rules for extraordinary vertices & boundaries

The rule presented above works only for regular triangular meshes. New rule has to be derived such that the limit surface near extraordinary vertices and along boundaries is at least C^1 continuous.

5.1. Extraordinary vertices

In case of extraordinary vertex we use the method presented in [7] to treat the problem. In the interpolatory $\sqrt{3}$ -subdivision, a new vertex q^{k+1} is computed by

$$q^{k+1} = \alpha p^k + \sum_{i=0}^{n-1} \alpha_i p_i^k, \quad (12)$$

where p^k is the extraordinary vertex of the mesh M_k , $\{p_i^k\}_{i=0}^{n-1}$ is the neighbor set of p^k , n is the valence of p^k , and α, α_i are the weights of p^k, p_i^k respectively. The subdivision matrix S over the extraordinary vertex p^k is a

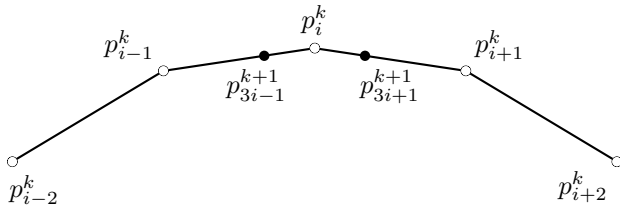


Figure 4. Curve subdivision rules along the boundary edges

$(n+1) \times (n+1)$ matrix. With the help of sophisticated eigen-analysis of $\tilde{S} = RSS$ similar to the regular case, we get the weights for a double step subdivision scheme as follows ($n \geq 5$):

$$\tilde{\alpha} = 8/9, \quad \tilde{\alpha}_i^n = \left\{ \frac{1}{9} + \frac{2}{3} \cos\left(\frac{2\pi i}{n}\right) + \frac{2}{9} \cos\left(\frac{4\pi i}{n}\right) \right\} / n,$$

for $n = 3$ we have

$$\tilde{\alpha} = 8/9, \quad \tilde{\alpha}_0^3 = 7/27, \quad \tilde{\alpha}_1^3 = \tilde{\alpha}_2^3 = -2/27,$$

and for $n = 4$ we take

$$\tilde{\alpha} = 8/9, \quad \tilde{\alpha}_0^4 = 7/36, \quad \tilde{\alpha}_1^4 = \tilde{\alpha}_3^4 = 1/36, \quad \tilde{\alpha}_2^4 = -5/36.$$

And the weight in matrix S is a suitable square root of S^2 which can be obtained by eigenvector analysis of S^2 . With these weights, the leading eigenvalues of \tilde{S} for $n \geq 5$ are

$$\lambda_0 = 1, \quad \lambda_1 = \lambda_2 = 1/3, \quad \lambda_3 = \lambda_4 = \lambda_5 = 1/9. \quad (13)$$

5.2. Boundary edges

No inner vertices should be involved in computation of boundary edge points, which means the boundary edge subdivision rule should be a curve subdivision scheme other than a surface one.

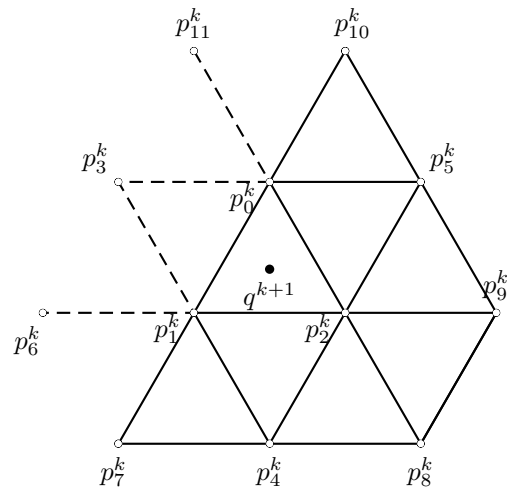


Figure 5. 'Virtual' points near boundary of the mesh

Splitting a boundary edge into three parts in every two steps of subdivision, we use the rules proposed in [7]. Two vertices are inserted on the edge using the stencil which contains 4 points (See Figure 4). The scheme leads to C^1 boundary curves.

The subdivision rules are

$$p_{3i-1}^{k+1} = -\frac{4}{81} p_{i-2}^k + \frac{10}{27} p_{i-1}^k + \frac{20}{27} p_i^k - \frac{5}{81} p_{i+1}^k$$

$$p_{3i+1}^{k+1} = -\frac{5}{81} p_{i-1}^k + \frac{20}{27} p_i^k + \frac{10}{27} p_{i+1}^k - \frac{4}{81} p_{i+2}^k.$$

5.3. Boundary triangles

For the case of boundary triangles, ‘virtual’ points [7] might be used to construct the entire stencil which are computed as follows:

$$\tilde{p}_3^k = p_0^k + p_1^k - p_2^k, \quad \tilde{p}_6^k = 2p_1^k - p_2^k, \quad \tilde{p}_{11}^k = 2p_0^k - p_2^k.$$

where points $\tilde{p}_3^k, \tilde{p}_6^k, \tilde{p}_{11}^k$ are ‘virtual’ points that lie outside the mesh (See Figure 5). By applying the regular subdivision rule on this modified stencil, new face point is added to the boundary triangle where each inner vertex has valence 6. If the valence of the vertex is not 6, the rule for extraordinary vertex is implemented.

6. Examples

We applied our subdivision scheme to several examples. The parameter α in our models is set to be -0.045 , though other choice might be used in practical applications. Figure 6 shows the resulting mesh of a 2-Torus model using classical Butterfly scheme (6.b) and our subdivision scheme (6.c). We see that a fair number of creases appear in (6.b) while they disappear when using our scheme.

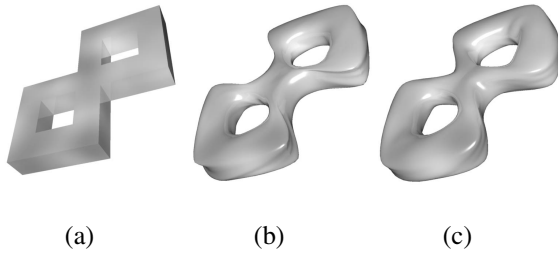


Figure 6. Subdivision comparison over a 2-torus model. Images from left to right are: initial mesh(a); 4-step Butterfly resulting mesh(b); our scheme after 5 steps(c). Here we see considerable wrinkles appear after using Butterfly scheme(b), while they disappear in our scheme(c).

Another example is Doraemon model. We compare the interpolatory- $\sqrt{3}$ scheme with our subdivision scheme based on PB-splines(See Figure 7). The two schemes lead to the same mesh size with 304236 vertices and 608472 triangles. (7.b) and (7.c) show the resulting meshes along with some local details. Here we see that our method has more powerful capability to handle the sharp characters such as the mouth corner.

We also apply our scheme to some other models. Figure 8 shows the resulting mesh of famous Venus model and Table 1 shows the Gaussian curvature distributions (and

other details) of these schemes, from which we see our new scheme demonstrate more advantages against Butterfly scheme - much less wrinkles, lower curvature bound and lower curvature variance.

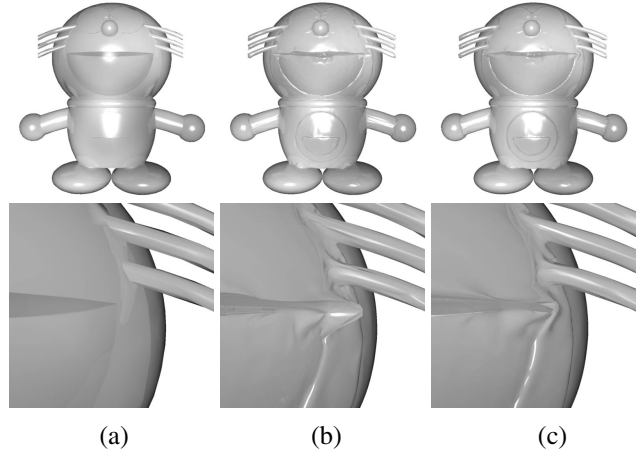


Figure 7. Famous cartoon character Doraemon model. (a) is the coarse mesh; (b) is 4-step interpolatory- $\sqrt{3}$ resulting surface and (c) is resulting mesh of our scheme after 4 steps. More details on the mouth corner are shown as well.

Model		V	T	GI	GA	GV	GR
1	Btfly(4)	8k	17k	-1.2	2.3	0.6	0.6
	Our(5)	8k	16k	-0.6	1.3	0.3	0.3
2	I- $\sqrt{3}$ (4)	304k	608k	-26.4	29.3	1.4	9.3
	Our(4)	304k	608k	-21.5	23.7	1.1	7.5
3	I- $\sqrt{3}$ (5)	172k	344k	-3.8	5.7	0.9	1.6
	Our(5)	172k	344k	-2.6	4.2	0.8	1.1

Table 1. Subdivision methods comparison via Gaussian curvature distribution. The columns from left to right are: Model (1: 2Torus, 2: Doraemon, 3: Venus), Subdivision Type (Number), Vertices, Triangles, Gaussian curvature mInimum/mAXimum/aVerage/vaRiance.

7. Conclusions & future work

We have derived a new interpolatory subdivision scheme for triangle meshes based on PB-splines. It can produce various smooth surfaces and lead to C^0, C^1 or C^2 smooth

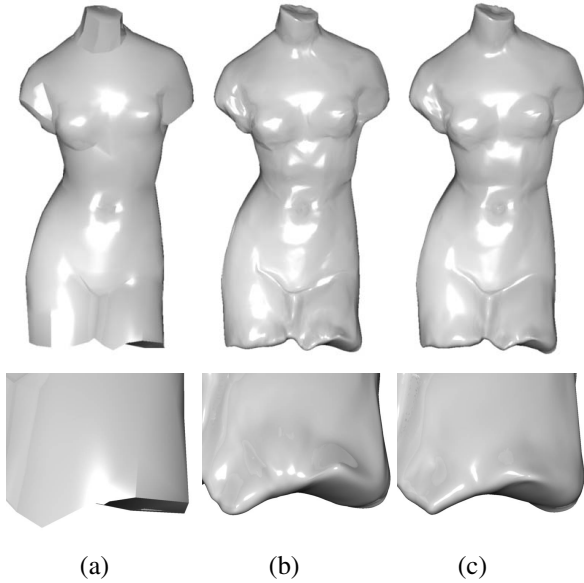


Figure 8. Subdivision Surfaces from Venus model. (a) is the original mesh with 711 vertices and 1418 triangles; (b) is the resulting surface after 5 steps of interpolatory- $\sqrt{3}$ scheme and (c) is the surface after 5 steps of our scheme, details on the sharp characters are shown in smaller pictures.

surfaces by applying different values of a parameter α to each regular vertex.

By using 1-to-9 split in every other step instead of 1-to-4 split which is commonly used in methods of triangular subdivision, only three new triangles are computed out of a coarse triangle in each step. Therefore the growth of mesh size is reduced compared to the normal 1-to-4 split and more refinement levels can be computed before the mesh reaches the prescribed complexity.

By far we only apply parameter α on regular vertices (valence=6) to refine triangle meshes. It's believable that $\alpha(n)$ with respect to the valence n , may be obtained through further analysis of the subdivision stencil near extraordinary vertex. Although it's hard to get the analytic expression of $\alpha(n)$, numerical value or approximation of $\alpha(n)$ might be reasonably investigated from which new subdivision refinement rules over irregular vertices may be available.

Another open question is how to decide accurate α based on local curvature. Examples in this paper use uniform value of -0.045 , but other choices should be explored in practical designs.

Acknowledgement

The authors are support by the Outstanding Youth Grant of NSF of China (No.60225002), a National Key Basic Research Project of China (2004CB318000), NSF of China (No. 10201030 and 60473132), the TRAPOYT in Higher Education Institute of MOE of China, and SRF for ROCS, SEM.

References

- [1] E. Catmull and J. Clark. Recursively generated b-spline surfaces on arbitrary topological meshes. *CAD*, 10:350–355, 1978.
- [2] R. Clough and J. Tocher. Finite element stiffness matrices for analysis of plates in bending. In *Proc. of Conference on Matrix Methods in Structure Mechanics*, pages 515–545, Wright-Patterson Air Force Base, 1965.
- [3] D. Doo and M. Sabin. Behaviour of recursive division surfaces near extraordinary points. *Computer-Aided Design*, 10:356–360, 1978.
- [4] N. Dyn, D. Levin, and J. Gregory. A butterfly subdivision scheme for surface interpolation with tension control. *ACM Trans. Graph.*, 9:160–169, 1990.
- [5] L. Kobbelt. Interpolatory subdivision on open quadrilateral nets with arbitrary topology. *Computer Graphics Forum*, 15:C409–420,C485, 1996.
- [6] L. Kobbelt. $\sqrt{3}$ -subdivision. *Proceedings of SIGGRAPH 2000*, pages 103–112, 2000.
- [7] U. Labsik and G. Greiner. Interpolatory $\sqrt{3}$ -subdivision. *Comput. Graph. Forum*, 19, 2000.
- [8] M.-J. Lai and L. L. Schumaker. Macro-elements and stable local bases for splines on clough-tocher triangulations. *Numer. Math.*, 88:105–119, 2001.
- [9] C. Loop. Smooth subdivision surfaces based on triangles. Master's thesis, Utah University, 1987.
- [10] T. W. Sederberg, J. Zheng, A. Bakenov, and A. H. Nasri. T-splines and t-nurccs. *ACM Trans. Graph.*, 22(3):477–484, 2003.
- [11] J. Warren and H. Weimer. *Subdivision Methods for Geometric Design: A Constructive Approach*. Morgan Kaufmann Publishers, October 2001.